ACS APPLIED MATERIALS & INTERFACES

Research Article

www.acsami.org

Perfluorocarbon-Encapsulated PLGA-PEG Emulsions as Enhancement Agents for Highly Efficient Reoxygenation to Cell and Organism

Yanjie Yao,[†,▽] Minmin Zhang,[§,▽] Tian Liu,[†] Juan Zhou,[‡] Yuan Gao,[§] Zhengfeng Wen,[∥] Jun Guan,[∥] Jun Zhu,[*,‡,⊥] Zhaofen Lin,[*,∥] and Dannong He[*,†,‡,⊥]

[†]School of Materials Science and Engineering, Shanghai Jiao Tong University, 800 Dongchuan Road, Shanghai 200240, P. R. China

[‡]National Engineering Research Center for Nanotechnology, 28 East Jiang Chuan Road, Shanghai 200241, P. R. China

[§]Department of Gastroenterology, ChangHai Hospital, Second Military Medical University, Shanghai 200433, P. R. China

[∥]Department of Emergency and Critical Care Medicine, Shanghai Changzheng Hospital, Second Military Medical University, Shanghai 200003, P. R. China

[⊥]Key Laboratory of Organofluorine Chemistry, Shanghai Institute of Organic Chemistry, Chinese Academy of Sciences, Shanghai 200032, P. R. China

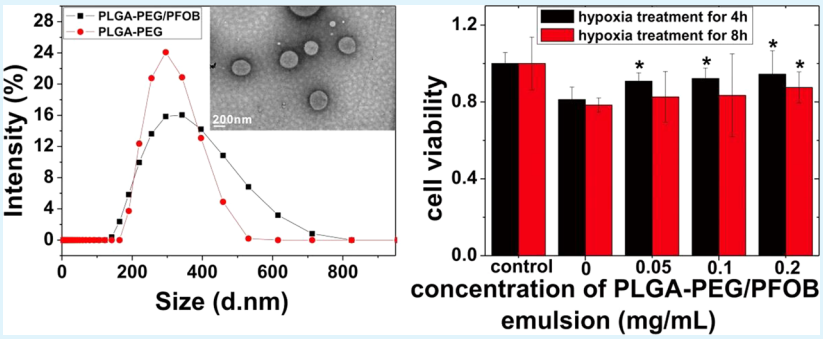

ABSTRACT: Perfluorocarbon (PFC), a kind of oxygen carrier, is encapsulated in PLGA-PEG to prepare a PLGA-PEG/PFC emulsion for highly efficient reoxygenation to cell and organism. HCT 116 cells are used as a model cell, whose viability has a significant enhancement after reoxygenation with PLGA-PEG/PFC emulsion because of the sufficient and timely oxygen supply. Meanwhile, hypoxia-reoxygenation injury will happen along with cell hypoxia-reoxygenation treatment, which is reflected by increasing reactive oxygen species (ROS) in cells. However, the integration of intracellular ROS and cell viability implies that the degree of hypoxia-reoxygenation injury is sublethal to HCT116 cells when the concentration of PLGA-PEG/PFC emulsion is lower than 0.2 mg/mL. Furthermore, the change of the expression level of hypoxia-inducible factor-1α (HIF-1α) is similar to that of cell viability during reoxygenation, which suggests that HIF-1α or its downstream proteins may make a significant contribution to cell viability. *In vivo* oxygen supply is assessed in rats through pulmonary delivery, which shows that PLGA-PEG/PFC emulsion can supply oxygen to rats and improve rats' lung ventilation.

KEYWORDS: *perfluorocarbon emulsion, hypoxia-reoxygenation, ROS, HIF-1α, pulmonary delivery*

INTRODUCTION

Artificial oxygen carriers, including perfluorocarbon emulsion, hemoglobin-based carrier, synthetic heme, and its polymer metal complexes, have attracted increasing attention due to their ability in dissolving and delivering oxygen.[1−6] However, although most of the perfluorocarbon emulsion could not be applied as blood substitutes until now, their application in medicine is still continued because of their therapeutic effect, which would be used on potential clinical care, such as cancer diagnosis, organ transplantation, and prevention of ischemia/reperfusion injury of tissues and organs.[7−14] For example, Jia et al.[7] reported perfluoropentane-encapsulated hollow mesoporous prussian blue nanocubes for activated ultrasound imaging and photothermal therapy of cancer. Marada et al.[13] used perfluorocarbon to improve post-transplant survival and early kidney function following prolonged cold ischemia. However, few reports have focused on the effect of oxygen in perfluorocarbon emulsion on the physiological characteristics of cell and/or organism during the therapy using perfluorocarbon emulsion.

As is well-known, oxygen is a key parameter in maintaining cell viability and functionality,[4] and cellular necrosis inevitably follows extended periods of anoxia or severe hypoxia. In the past years, there are many researchers concentrating on the study of the changes of cellular homeostasis, especially on intracellular signal expression during hypoxia and reoxygena-

Received: May 15, 2015
Accepted: July 29, 2015
Published: July 29, 2015

DOI: 10.1021/acsami.5b04226
ACS Appl. Mater. Interfaces 2015, 7, 18369−18378

Scheme 1. Schematic Illustration of PLGA-PEG/PFOB Emulsion Preparation and Its Interaction with HCT116 Cell on the Condition of Hypoxia and Reoxygenation

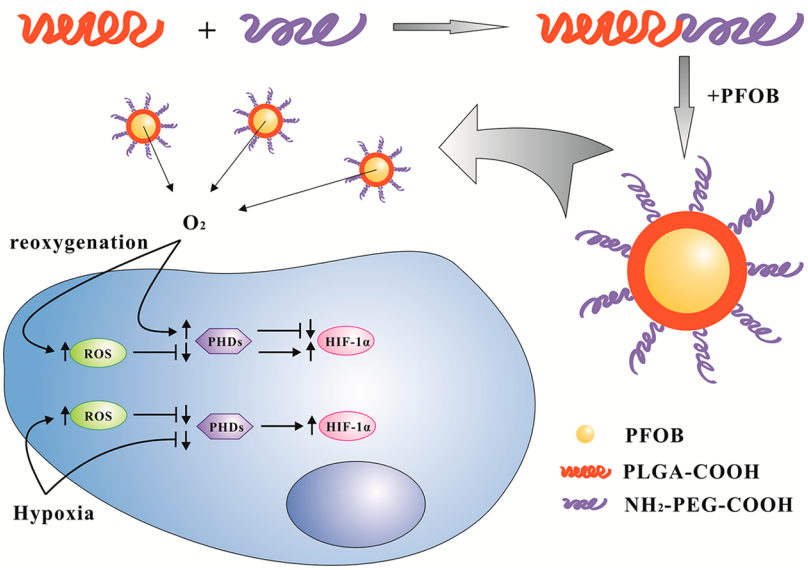

tion.[15−21] Some typical parameters, including reactive oxygen species (ROS), hypoxia-inducible factor (HIF), NADPH oxidases, and so on, have been explored to characterize a cell state at the condition of oxygen deficit and/or rich. For examples, Guzy et al.[16] showed that ROS production was specifically required for hypoxia-induced HIF-α stabilization during hypoxia. Luo et al.[20] demonstrated that hypoxia/reoxygenation-promoted human major histocompatibility complex class I-related chain A (MICA) expression on HK-2 cells is through a HIF-1 pathway. Among them, the condition of hypoxia always comes from environmental hypoxia or chemical simulated hypoxia, and the condition of reoxygenation is always attributed to normoxia. However, few researchers have paid attention to intracellular signal expression using perfluorocarbon emulsion as a hypoxia-reoxygenation treatment.

On the other hand, the lung is an important organ for oxygen exchange, although the oxygen supply of perfluorocarbon emulsion is applied by the intravenous injection. Furthermore, the lung is also an attractive target for drug delivery due to noninvasive means to provide not only local lung effects but possibly high systemic bioavailability, avoidance of first-pass metabolism, more rapid onset of therapeutic action, and the availability of a huge surface area.[22,23] Therefore, it is currently believed that drug delivery into the human lung represents the best way to treat pulmonary diseases. As a consequence, many kinds of nanocarriers have been developed for pulmonary drug delivery, such as liposomes, microemulsions, micro- and nanoparticles, cyclodextrins, and so on. Among them, a biodegradable polymer carrier, PLGA particles, has generated tremendous research interest due to their excellent biocompatibility and efficient transport to the target when adequately engineered as well as the possibility of tailoring their biodegradability by varying the composition (lactide/glycolide ratio), molecular weight, and chemical structure.[24−26] For example, Takami et al.[27] prepared PEG-PLA/PLGA microspheres for pulmonary drug delivery by a novel emulsification technique assisted with amphiphilic block copolymers. Yang et al.[28] reported a new route to make highly porous large polymeric microparticles for local drug delivery. Martin-Banderas et al.[29] used flow focusing technology to produce tobramycin-loaded PLGA microspheres for pulmonary drug delivery. Nonetheless, PFC encapsulated in PLGA as an oxygen carrier was rarely used for pulmonary delivery to supply oxygen.

In the present work, on the basis of the good properties of PEG which can both render the carriers unrecognizable to phagocytes and reduce the aggregation of the carriers,[30] we use PEGylated PLGA as a carrier to prepare PLGA-PEG/PFOB (PFOB, a kind of PFC with wide application in clinic[31−33]) emulsion and apply as an oxygen carrier to supply oxygen. To evaluate the effect of PLGA-PEG/PFOB emulsion on cells, the cell viability, intracellular ROS production, and expression of HIF-1α are detected on the condition of hypoxia, reoxygenation, and reoxygenation with the emulsion. The emulsion preparation and the interaction with cell are schematically illustrated in Scheme 1. Furthermore, *in vivo* oxygen supply is assessed in rats through pulmonary delivery. The results of *in vitro* and *in vivo* experiments show its capacity to supply oxygen to the cell and organism, which implies that the emulsion may have potential to ease hyoxemia in the future. The research also provides a new mode of administration on pulmonary delivery for artificial oxygen carriers in biomedical applications.

EXPERIMENTAL SECTION

Materials. Poly(lactide-*co*-glycolide) Resomer RG502 (PLGA-COOH, MW 20,000) was purchased from Jinan Daigang Biomaterial Co., Ltd. Amine-PEG-carboxymethyl (NH_2-PEG-COOH, MW 3400) was purchased from Shanghai Seebio Biotech, Inc. 2′,7′-Dichlorofluorescin diacetate and perfluoroctyl bromide (PFOB, 99%) were purchased from Sigma. All chemical reagents were analytical grade or above and purchased from Sinopharm Chemical Reagent Co., Ltd. Triethylamine and dichloromethane were dried with calcium hydride before use. The HCT116 cell line was purchased from the cell bank of Chinese Academy of Sciences, and the cultivate reagents were purchased from Life Technologies (Gibco, USA). Cell counting kit-8 (CCK-8) was purchased from Beijing Fanbo Biochemicals Co., Ltd. All reagents of Western blot analysis were purchased from Shanghai Weiao BioTech Co., Ltd. The rats were purchased from an experimental animal center of Second Military Medical University, and the nude mice were purchased from an experimental animal center of Shanghai Jiao Tong University.

Synthesis of PLGA-PEG Macromolecule. Carboxylate-functionalized copolymer PLGA-PEG was synthesized by the conjugation of

DOI: 10.1021/acsami.5b04226
ACS Appl. Mater. Interfaces 2015, 7, 18369−18378

PLGA-COOH to NH_2-PEG-COOH. A total of 1 g of PLGA-COOH, 9 mg of *N*-hydroxysuccinimide (NHS), 14.5 mg of 1-(3-(dimethylamino)propyl)-3-ethylcarbodiimide hydrochloride (EDC), and 5 mg of 4-dimethylaminopyridine (DMAP) were dissolved in 10 mL of dichloromethane and stirred for 24 h at room temperature to convert PLGA-COOH to PLGA-NHS. Then, 170 mg of NH_2-PEG-COOH and 43 μL of triethylamine were added into the solution. After further stirring for 8 h, dichloromethane was removed through a rotary evaporator and 5 mL of DMF was added to dissolve the product. Then, the solution was added to a dialysis bag (the width is 44 mm, and the molecular weight cutoff is 8000−14000) and unreacted PEG and other small molecules were removed by dialyzing for 3 days. Then, the product was freeze-dried for 24−48 h. The samples were measured by ^{1}H nuclear magnetic resonance to verify the response rate.

Synthesis of PLGA-FITC. A total of 300 mg of PLGA-COOH, 1.8 mg of NHS, 2.9 mg of EDC, and 1 mg of DMAP were dissolved in 10 mL of dichloromethane and stirred for 24 h at room temperature to convert PLGA-COOH to PLGA-NHS. Then, 1.8 mg of ethylenediamine and 8.6 μL of triethylamine were added into the solution. After further stirring for 3 h, 35 mg of FITC was added into the solution and left to stir for 8 h. Then, dichloromethane was removed through a rotary evaporator and 5 mL of DMF was added to dissolve the product. After that, the solution was added to a dialysis bag (the width is 44 mm, and the molecular weight cutoff is 8000−14000) and unreacted FITC and other small molecules were removed by dialyzing for 3−5 days. Then, the product was freeze-dried for 24−48 h.

Preparation of PLGA-PEG/PFOB Emulsion. PLGA-PEG/PFOB emulsion was prepared by modifying the solvent emulsion/evaporation method to obtain capsules with a polymeric shell encapsulating perfluorooctyl bromide (PFOB), similar to what was previously described.[34−36] Briefly, 10 mg of PLGA-PEG was dissolved into 200 μL of dichloromethane along with the desired amount of PFOB and 200 μL of 15% Span80@dichloromethane (w/v). After well blended, the organic solution was then emulsified into 2 mL using an Ultraturrax T10 (IKA) to form a pre-emulsion, and emulsification was performed in a 15 mL centrifuge tube placed over ice for 1 min. Then, the pre-emulsion was sonicated with a vibrating metallic tip, JY 92-IIN (SCIENTZ, China), for 3 min over ice. It works for 3 s, then stops for 10 s, and repeats the process under 50% power (300 w). After further stirring with Ultraturrax T10 (IKA) for 10 min (works 1 min and stops 1 min) over ice, organic solvents were then evaporated by magnetic stirring for about 3 h at room temperature. For contrast, PLGA-PEG emulsion without PFOB was prepared in the same process. In addition, PLGA-PEG mixed with 50% PLGA-FITC was used to prepare the emulsion with fluorescence for *in vivo* biodistribution imaging.

Characterizations. Particle size and zeta potential were measured by a Malvern Zetasizer Nano ZS (Malvern Instruments Ltd., Malvern, Worcestershire, U.K.) based on dynamic light scattering. The ^{1}H nuclear magnetic resonance (NMR) spectra were recorded on a Bruker AM-400 spectrometer in $CDCl_3$ solution at room temperature. Transmission electron microscopy (TEM) images were recorded on a JEOL-2100F instrument using an accelerating voltage of 200 kV. Fourier transform infrared spectroscopy (FT-IR) of PFOB, PLGA-PEG emulsion, and PLGA-PEG/PFOB emulsion was investigated on a Nicolet 6700 FT-IR spectrometer. Fluorine content was determined by high performance ion chromatography (Dionex 500, USA) with conductivity detection through oxygen flask combustion (separating column, IonPac AG_{14}-AS_{14}; eluent, 0.0010 M $NaHCO_3$ + 0.0035 M Na_2CO_3). *In vivo* biodistribution imaging was performed on a Caliper IVIS Lumina II imaging system (Caliper Life Sciences, USA).

Cell Cytotoxicity. Cells were cultured in 37.5 cm^2 flasks in DMEM containing 10% fetal bovine serum (FBS) and 1% antibiotics at a humidified, 37 °C, and 5% CO_2 incubator. The cytotoxic effects of PLGA-PEG/PFOB emulsion were determined with the CCK-8 assay.[37−39] Briefly, HCT 116 cells were seeded at a density of 5000 cells per well in 96-well plates. After 48 h, the medium was replaced with 100 μL of medium with different concentrations of PLGA-PEG/PFOB or PLGA-PEG emulsion, but control cells were incubated with DMEM medium alone. After incubation for 4, 8, 12, and 24 h, the supernatant was removed and 10 μL of CCK-8 solutions were added to each well of the plate (total medium 100 μL/well). Then, cells were incubated at 37 °C. After 4 h of incubation, absorbance was measured using an iMark Microplate Reader (Bio-Rad, USA) at 450 nm as the measure wavelength.

Cell Viability during Hypoxia-Reoxygenation Treatment. HCT 116 cells were seeded at a density of 5000 cells per well in 96-well plates. After 48 h, the medium was replaced with 100 μL of DMEM without FBS, and then, 100 μL of liquid paraffin was added to each well of the plate except for the control group. Because of its low density and highly hydrophobic nature, liquid paraffin formed a film over the medium. As a consequence, the medium was separated from the normoxic atmosphere by the overlying liquid paraffin film, which provided a hypoxic environment to the cell culture. After incubation under hypoxia condition for 4 and 8 h, liquid paraffin and DMEM were removed and 100 μL of medium with 10% FBS and different concentrations of PLGA-PEG/PFOB or PLGA-PEG emulsion was added for 2 h reoxygenation. Finally, cell viability was determined with the CCK-8 assay.

Measurement of ROS. Intracellular reactive oxygen species (ROS) generation was measured by 2′,7′-dichlorofluorescin diacetate (DCFH-DA). After cellular uptake of DCFH-DA, it was cleaved by cellular esterases to 2′,7′-dichlorofluorescin (DCFH), and then, the intracellular ROS would cause the oxidation of DCFH to the fluorescent product of 2′,7′-dichlorofluorescein (DCF). Cells plated on 6-well cell culture plates were maintained under hypoxic conditions for 12 h, and then, DMEM was replaced with the medium containing different concentrations of PLGA-PEG/PFOB emulsion for 2 h of reoxygenation, after which cells were washed and incubated with DCFH-DA (10 μM) in serum-free culture medium under normoxic condition for an additional 30 min. The medium was removed, and cells were washed three times with PBS. The DCF fluorescence intensity was measured using fluorescence microscopy excited by blue light, and also detected by a flow cytometer with an excitation wavelength of 488 nm after cells should be digested with trypsin enzyme first and washed three times with PBS through a centrifuge (1000 rpm, 3 min, 4 °C).

Western Blot Analysis. Hypoxia-inducible factor-1α (HIF-1α) was detected by Western blot analysis. Cell hypoxia-reoxygenation treatment was similar to that of measurement of ROS. Whole-cell lysates were generated by washing cells with PBS three times and then lysing attached cells with RIPA lysis buffer containing freshly added 1 nM PMSF. The whole process was carried out in the ice, and reagents were precooled in 4 °C. Extracts were then centrifuged at 12 000 rpm and 4 °C for 5 min, and the supernatant was collected for the determination of the protein concentration (BCA protein assay). After the protein concentration of every sample was adjusted to a constant (2 μg/μL), the protein was mixed with SDS-PAGE loading buffer, boiled for 5 min, and stored at −80 °C. Protein extracts were run at 100 V on a SDS-PAGE gel and transferred to a polyvinylidene fluoride membrane at 100 V for 70 min, and the membranes were blocked with TBS + 0.1% Tween-20 (TBS-T) + 3% BSA for 1 h at room temperature. Furthermore, the HIF-1α primary antibody was added to TBS-T + 3% BSA (dilution 1:200) and incubated with the membrane for 1 h at room temperature overnight at 4 °C. After the membranes were washed with TBS-T, the secondary antibody conjugated with HRP was added to the membrane with TBS-T for 2 h at room temperature, which was detected by chemiluminescence. For detection of β-actin, the membrane was stripped and β-actin antibody was added with a dilution of 1:500. HIF-1α blots were quantified via densitometric analysis and normalized to β-actin levels.

***In Vivo* Oxygen Supply.** The animal study was approved by the institutional review board for animal research. *In vivo* oxygen supply through pulmonary delivery was assessed in rats, which was separated into two groups. The control group was instilled with 0.9% NaCl, and the experimental group was instilled with PLGA-PEG/PFOB emulsion from trachea. The effects of the instillment on rats' ventilation were reflected by the PO_2 (partial pressure of oxygen) and PCO_2 (partial pressure of carbon dioxide) in carotid artery blood. Anesthesia was performed by intraperitoneal injection with 3% nembutal at a rate of

DOI: 10.1021/acsami.5b04226
ACS Appl. Mater. Interfaces 2015, 7, 18369−18378

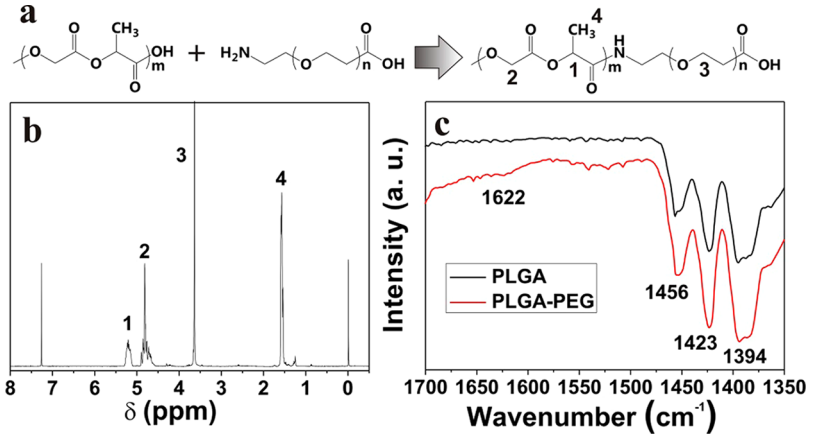

Figure 1. (a) Synthesis scheme, (b) ^{1}H NMR of PLGA-PEG, and (c) FT-IR of PLGA-PEG and PLGA.

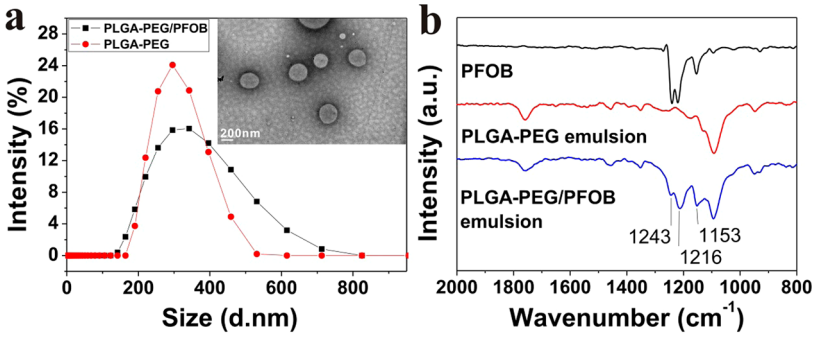

Figure 2. (a) Size distribution of PLGA-PEG emulsion and PLGA-PEG/PFOB emulsion and (b) FT-IR spectra of PFOB, PLGA-PEG emulsion, and PLGA-PEG/PFOB emulsion. The inset is a TEM image of PLGA-PEG/PFOB emulsion.

0.2 mL per 100 g. And rats were instilled with 0.3 mL of emulsion or 0.9% NaCl from trachea at a speed of 0.1 mL/min. About 0.3 mL of heparin, used to avoid blood coagulation and supply fluid, was injected after 0.3 mL of carotid artery blood was drawn to blood gas analysis. Rats were dissected to observe the lung injury after experiment.

***In Vivo* Biodistribution of PLGA-PEG/PLGA-FITC/PFOB Emulsion.** Nude mice were used to evaluate *in vivo* biodistribution of PLGA-PEG/PFOB emulsion. Anesthesia was performed by intraperitoneal injection with 5% chloral hydrate at a mouse of 0.1 mL per 10 g. About 0.05 mL of PLGA-PEG/PLGA-FITC/PFOB emulsion was instilled from trachea at a speed of 0.1 mL/min. *In vivo* biodistribution imaging was performed every 1 h. Finally, the mice were anatomized to confirm the organ type.

Statistical Analysis. Results are expressed as the mean ± standard deviation (SD). Statistical analysis was done using a Student's *t* test. Differences were considered significant at a *P* value of <0.05.

RESULTS AND DISCUSSION

The PLGA-PEG macromolecules were synthesized by conjugating activated PLGA-COOH and NH_2-PEG-COOH through EDC/NHS coupling chemistry. The whole procedure is schematically illustrated in Figure 1a. The structure of the obtained product is characterized by ^{1}H nuclear magnetic resonance (^{1}H NMR). As shown in Figure 1b, the conjugation of PLGA-COOH and NH_2-PEG-COOH is confirmed by ^{1}H NMR analysis of a polymer solution in $CDCl_3$: (δ; ppm): 5.2 (H1 from PLGA-COOH), 4.8 (H2 from PLGA-COOH), 3.7 (H3 from NH_2-PEG-COOH), and 1.6 (H4 from PLGA-COOH), which shows the successful synthesis of PLGA-PEG. Furthermore, on the basis of a previous report,[35] the efficiency of the coupling reaction is calculated as follows: In our experiment, the molecular weight of PLGA monomer is 130, and the molecular weight of PLGA is about 20 000. Thus, the PLGA macromolecule includes about 154 monomers, in which there are two H2 atoms. Similarly, the PEG macromolecule in our experiment includes about 77 monomers, in which there are four H3 atoms. Therefore, the quantity of H2 atoms in PLGA macromolecule is equal to that of H3 atoms in PEG macromolecule. If PLGA was conjugated with PEG completely, the ^{1}H NMR peak area of H3 atoms in PEG macromolecule and H2 atoms in PLGA macromolecule would be equal. However, on the basis of unreacted PEG being removed by dialyzing, the peak area of H3 atoms in PEG macromolecule and H2 atoms in PLGA macromolecule is 4.00 and 4.44, respectively, whose ratio is 4.00/4.44 ≈ 90%. Therefore, we suggest that the efficiency of the coupling reaction is about 90%. Furthermore, FT-IR spectra were performed to characterize the synthesis of PLGA-PEG macromolecule. As shown in Figure 1c, the typical peaks of PLGA are shown at bands of 1456, 1423, and 1394 cm^{-1}, which should contribute to the absorption of −CH, $-CH_2$, and $-CH_3$ groups, respectively. Besides the above bands in PLGA-PEG FT-IR spectra, a weak new peak at 1622 cm^{-1} is found, which results from the absorption of amide bonds. The result indicates the successful covalent conjugation between PLGA and PEG.

Furthermore, PLGA-PEG/PFOB emulsions based on PLGA-PEG macromolecules are prepared. Figure 2a shows that the average hydrodynamic size of the PLGA-PEG and PLGA-PEG/PFOB emulsion in deionized water is about 282.1 and 302.3 nm, respectively, which reveals the PFOB addition has little influence on the size of the emulsion. Moreover, the inserted TEM image shows PLGA-PEG/PFOB emulsions with core in

DOI: 10.1021/acsami.5b04226
ACS Appl. Mater. Interfaces 2015, 7, 18369−18378

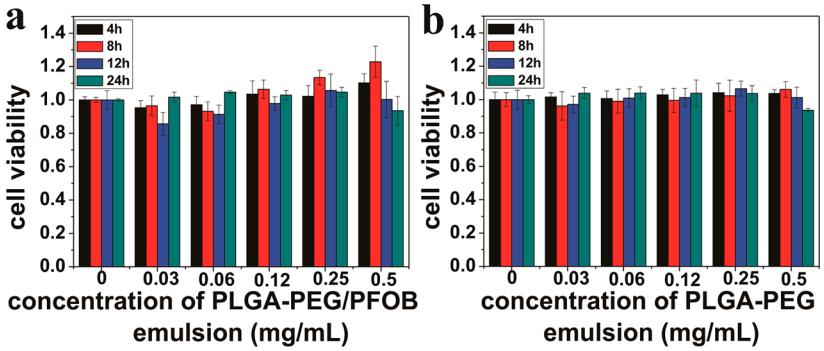

Figure 3. *In vitro* cell cytotoxicity of (a) PLGA-PEG/PFOB emulsion and (b) PLGA-PEG emulsion (concentration was calculated by PLGA-PEG).

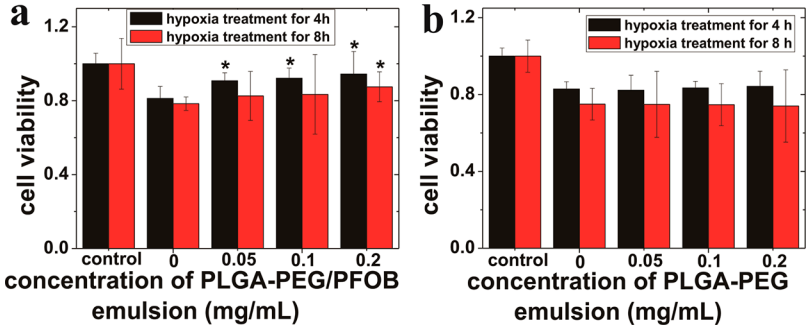

Figure 4. Cell viability on the condition of reoxygenation with (a) PLGA-PEG/PFOB emulsion and (b) PLGA-PEG emulsion after hypoxia treatment for 4 and 8 h (concentration was calculated by PLGA-PEG). The control group is cultured under normoxic condition with normal medium all along. *Significant differences compared to the group reoxygenation with normal medium ($P < 0.05$).

gray and shell in dark are uniform nanospheres with an average diameter of about 250 nm. Additionally, the addition of PFOB is further evidenced by FT-IR spectra (Figure 2b). In the spectra of PFOB, the —CF_2 group gives the characteristic stretching vibration bands at 1243 and 1216 cm^{-1}, whereas the stretching vibration band of the —CF_3 group is at 1153 cm^{-1}. Furthermore, in the spectra of PLGA-PEG emulsion, the band at 1095 cm^{-1} results from the absorption of C—C and C—O. In addition, the band at 1756 cm^{-1} is attributed to the absorption of C═O. Compared to the spectra of PFOB and PLGA-PEG/PFOB emulsion, the typical —CF_2 and —CF_3 peaks of PFOB can be obviously found in the spectra of PLGA-PEG/PFOB emulsion besides the typical peaks of PLGA-PEG emulsion, which suggests that PFOB has been encapsulated in PLGA-PEG emulsion successfully. Moreover, fluorine content in the freeze-dried powder of PLGA-PEG/PFOB emulsion is 10.43% determined by high performance ion chromatography. After conversion, PFOB content in the freeze-dried powder of PLGA-PEG/PFOB emulsion is 16.11%.

To evaluate the cytotoxicity characteristics of PLGA-PEG/PFOB emulsion, CCK-8 assays were performed. As shown in Figure 3a, the effect of varying concentrations (0.03−0.5 mg/mL) of PLGA-PEG/PFOB emulsion on the viability of HCT 116 cells after exposure for 4, 8, 12, and 24 h was investigated. The cell viability decreases with the addition of 0.03 mg/mL PLGA-PEG/PFOB emulsion but increases in the presence of 0.06−0.5 mg/mL PLGA-PEG/PFOB emulsion after exposure for 4, 8, and 12 h. About 110 and 123% cell viabilities are maintained even up to a relatively high dose of 0.5 mg/mL after exposure for 4 and 8 h, respectively. However, closer observation reveals that the cell viability is reduced to the level approximate to the control group at a concentration of 0.5 mg/mL at an incubation time of 12 h. Moreover, the cell viability almost has no changes after exposure for 24 h except at a concentration of 0.5 mg/mL and cell viability shows a little decrease but it is still more than 90%. The results show that PLGA-PEG/PFOB emulsion has a good biocompatibility and a little promotion to cell viability. Furthermore, to clarify the reason for the increasing cell viability, the cytotoxicity characteristics of PLGA-PEG emulsion were further performed. As shown in Figure 3b, there is no significant difference in cell viability with the increasing concentration of PLGA-PEG emulsion from 0.03 to 0.5 mg/mL compared to the control group ($P > 0.05$) except for the cell viability at a concentration of 0.5 mg/mL after exposure for 24 h, which shows a slight decline. These results suggest that the promotion to cell viability of PLGA-PEG/PFOB emulsion may be attributed to the addition of PFOB and the dissolving of oxygen in PFOB.

To estimate the reoxygenation ability of PLGA-PEG/PFOB emulsion, a hypoxia-reoxygenation treatment to HCT 116 cells was detected through the hypoxia-reoxygenation model with the liquid paraffin covering method. As shown in Figure 4a, cell viability is reduced after hypoxia treatment for 4 or 8 h, which is attributed to the poor cell states after hypoxia treatment, because cell viability cannot restore quickly after reoxygenation with a normal medium. Furthermore, when PLGA-PEG/PFOB emulsion is added, cell viability shows a significant enhancement compared to the group reoxygenation with normal medium ($P < 0.05$). However, the increasing concentration of PLGA-PEG/PFOB emulsion (0.05−0.2 mg/mL) has no significant inference to cell viability ($P > 0.05$). The reason for the enhancement in cell viability could lie in the high dissolved oxygen ability of PFOB, which supplies more oxygen to help cell reoxygenation to restore from the hypoxic state. In order to further prove the opinion, PLGA-PEG emulsion was used as a control for the hypoxia-reoxygenation treatment. The

DOI: 10.1021/acsami.5b04226
ACS Appl. Mater. Interfaces 2015, 7, 18369−18378

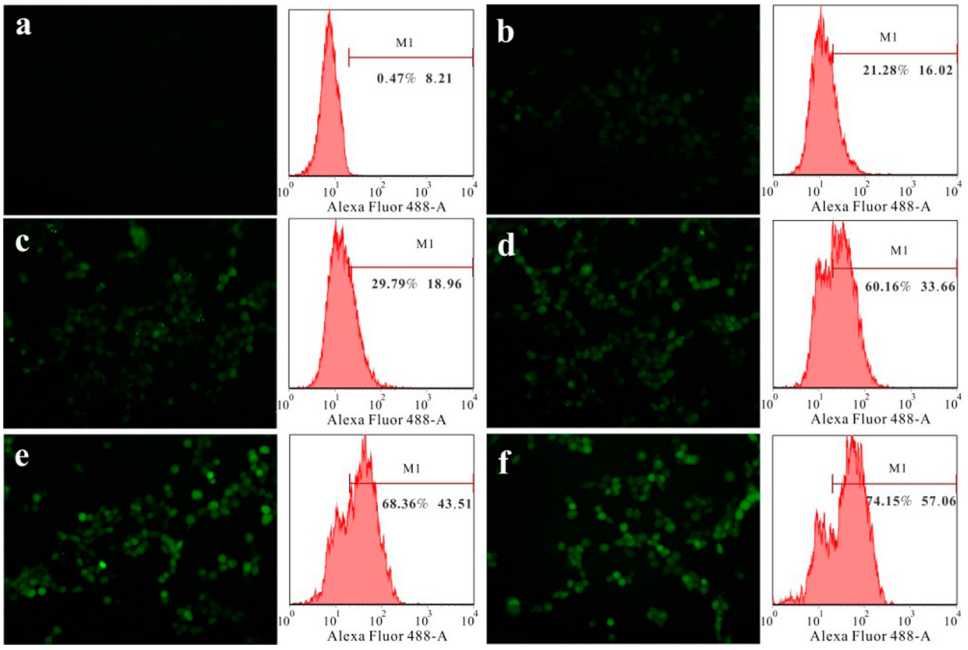

Figure 5. Fluorescent microscopic images and flow cytometry detection of cellular ROS production after hypoxia and reoxygenation treatment on the condition of (a) control group cultured under normoxia condition, (b) hypoxia treatment for 12 h, (c, d, e, and f) reoxygenation with PLGA-PEG/PFOB emulsion at a concentration of 0, 0.05, 0.1, and 0.2 mg/mL after hypoxia treatment for 12 h (concentration was calculated by PLGA-PEG).

addition of different concentrations of PLGA-PEG emulsion has no influence on cell viability ($P > 0.05$, Figure 4b). The results imply that the PLGA-PEG/PFOB emulsion can be used as an oxygen carrier to help cell reoxygenation through supplying oxygen to enhance cell viability.

As is well-known, reactive oxygen species (ROS) have been implicated in the regulation of many important cellular events including transcription factor activation, gene expression, and cellular proliferation. However, excessive production of ROS gives rise to the activation of events which could lead to cell injury or death. Furthermore, the previous reports also show that ROS production always accompanies cell hypoxia-reoxygenation treatment.[40−42] To explore the effect of PLGA-PEG/PFC emulsion on the ROS production during reoxygenation, ROS in HCT116 cells were measured by 2′,7′-dichlorofluorescin diacetate (DCFH-DA). There is almost no 2′,7′-dichlorofluorescein (DCF) fluorescence in the control group (Figure 5a), which implies that the ROS level in cells cultured under normoxia condition is very low. After 12 h of hypoxia treatment, green cells from DCF fluorescence can be seen in the fluorescent microscopic image (Figure 5b). Moreover, their intensity is further enhanced after reoxygenation treatment. As shown in Figure 5c−f, with the increase of the concentration of PLGA-PEG/PFOB emulsion for reoxygenation treatment, DCF fluorescent intensity is improved gradually, which implies that the ROS level in cells is also enhanced gradually. These results reveal that the hypoxic condition can result in ROS production in cells, the reoxygenation treatment can bring more excess ROS in cells, and the addition of PLGA-PEG/PFOB emulsion can further promote the ROS level in cells.

The result can also be concluded by flow cytometry detection. As shown in Figure 5, the main fluorescent intensities are continuously increased from 8.21 to 57.06 and the percentage of the DCF-positive cell in the M1 region is enhanced from 0.47 to 74.15% with the treatment of hypoxia, reoxygenation, and reoxygenation with PLGA-PEG/PFOB emulsion. The results suggest that the ROS level in cells was increased gradually during the ordinal treatment with different methods, which could contribute to the increasing oxygen concentration supplied by the PLGA-PEG/PFOB emulsion. On the other hand, the cell injury would suffer from these treatments because of the increasing ROS level. However, associated with the result of the increasing cell viability with the increasing PLGA-PEG/PFOB emulsion for hypoxia-reoxygenation treatment, we can suppose that this degree of hypoxia-reoxygenation injury is sublethal to HCT116 cells. The reason may be explained by the previous reports[18,19] as follows: though the production of ROS will cause cell hypoxia-reoxygenation injury, hypoxia-reoxygenation injury tolerance of various cell types differs, depending on the metabolic rate and intrinsic adaptive mechanisms of the cells.

In order to clarify the tolerance reason for HCT116 cells to ROS production during hypoxia-reoxygenation treatment, Western blot analysis was performed to examine the expression of hypoxia-inducible factor in cells. As is well-known, hypoxia-inducible factor-1 (HIF-1) is a transcription factor involved in homeostasis of oxygen concentration, which is the master regulator of cellular adaptive responses to hypoxia, and it may activate the transcription of more than 100 genes crucial for adaptation to hypoxia. HIF-1 is a heterodimer consisting of an α-subunit (HIF-1α) and β-subunit (HIF-1β), while HIF-1β protein is constitutively expressed; HIF-1α is O_2-regulated because it is degraded under normoxia following proline hydroxylation by prolyl hydroxylases (PHDs) which require O_2 as a substrate. In contrast, HIF-1α is stabilized under hypoxic conditions, and combines with HIF-1β, where it induces physiological responses to hypoxia by binding to the hypoxia response element in hypoxia responsive genes, activating transcription.[15−17,20,43] Thus, stabilization of HIF-1α can be

DOI: 10.1021/acsami.5b04226
ACS Appl. Mater. Interfaces 2015, 7, 18369−18378

seen as a crucial factor for cell viability during hypoxia as well as reoxygenation. Therefore, we evaluated the expression of HIF-1α during hypoxia and reoxygenation using β-actin as an internal control. As shown in Figure 6, the expression level of

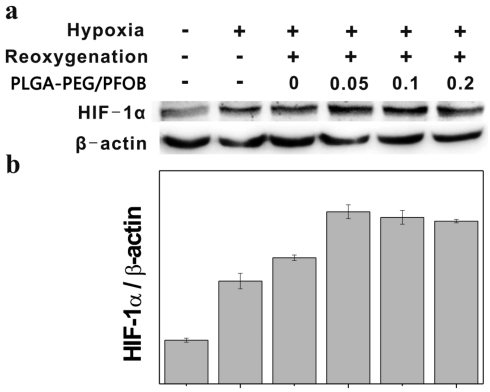

Figure 6. (a) Western blot analysis of HIF-1α and β-actin in HCT 116 cells under normoxic, hypoxia, and reoxygenation. (b) Densitometric analysis of HIF-1α normalized to β-actin.

HIF-1α in the control group cultured under normoxia condition is low because of the degradation by PHDs. After hypoxia treatment, it is up-regulated by more than 2-fold compared with the control group, and the following reoxygenation treatment can further enhance the expression level of HIF-1α. Moreover, the addition of PLGA-PEG/PFOB emulsion can significantly promote stabilization of HIF-1α during reoxygenation compared to the group reoxygenation with normal medium ($P < 0.01$). However, the increasing concentration of PLGA-PEG/PFOB emulsion (0.05–0.2 mg/mL) has no significant inference to the expression of HIF-1α ($P > 0.05$), which is similar to the result of cell viability after hypoxia-reoxygenation treatment. Thus, we can surmise the expression of HIF-1α may have an important contribution to cell viability during reoxygenation.

Previous reports[16,44] had demonstrated that mitochondrial release of ROS is required for hypoxic stabilization of HIF-1α, because ROS can affect the rate of HIF-1α hydroxylation, promoting HIF-1α accumulation and activation by partially inhibiting PHD activity. Though the regulation of PHDs by oxidant signals is poorly understood, it still shows the expression level of HIF-1α has an important relationship with the content of ROS. We have proved that the intracellular ROS level is enhanced gradually with the treatment of hypoxia, reoxygenation, and reoxygenation with PLGA-PEG/PFOB emulsion, but HIF-1α is not continuously increased as well as ROS when the concentration of PLGA-PEG/PFOB emulsion is increased. The reason may be explained as follows: the increase of oxygen concentration supplied by PLGA-PEG/PFOB emulsion enhances the activity of PHDs; thus, though the increasing content of ROS partially inhibits PHD activity, HIF-1α cannot further accumulate. Nevertheless, the expression level of HIF-1α is still much higher than the group reoxygenation without PLGA-PEG/PFOB emulsion.

To confirm the oxygen supply of PLGA-PEG/PFOB emulsion *in vivo*, a rat administration model was established, in which 10 mg/mL PLGA-PEG/PFOB emulsion was instilled through pulmonary delivery (Figure 7a) using 0.9% NaCl solution as the control group. The lung injury and the partial pressure of oxygen (PO_2) and carbon dioxide (PCO_2) were observed. As shown in Figure 7b and c, there is a large area of extravasated blood in lungs of the control group instilled with 0.9% NaCl, whereas little can be seen in lungs of the experimental group. The reason can be attributed to the following: the addition of surfactant reduces the surface tension so that the emulsion can better spread in the lungs, while high surface tension 0.9% NaCl may accumulate in some areas so as to cause blocking. Furthermore, the rats' carotid artery blood was drawn to blood gas analysis after intratracheal instillment. As shown in Figure 7d and e, PO_2 in both groups brings an obvious decrease after intratracheal instillment, which could mean that intratracheal instillment results in a temporary suffocation to rats. Then, PO_2 in the group instilled with PLGA-PEG/PFOB emulsion undergoes a continuous rise and finally achieves a value much higher than that before instillment (Figure 7e), while PO_2 in the control group stabilizes at a value close to the initial one after rise for the first 15 min (Figure 7d). The reason should be attributed to the oxygen dissolved in

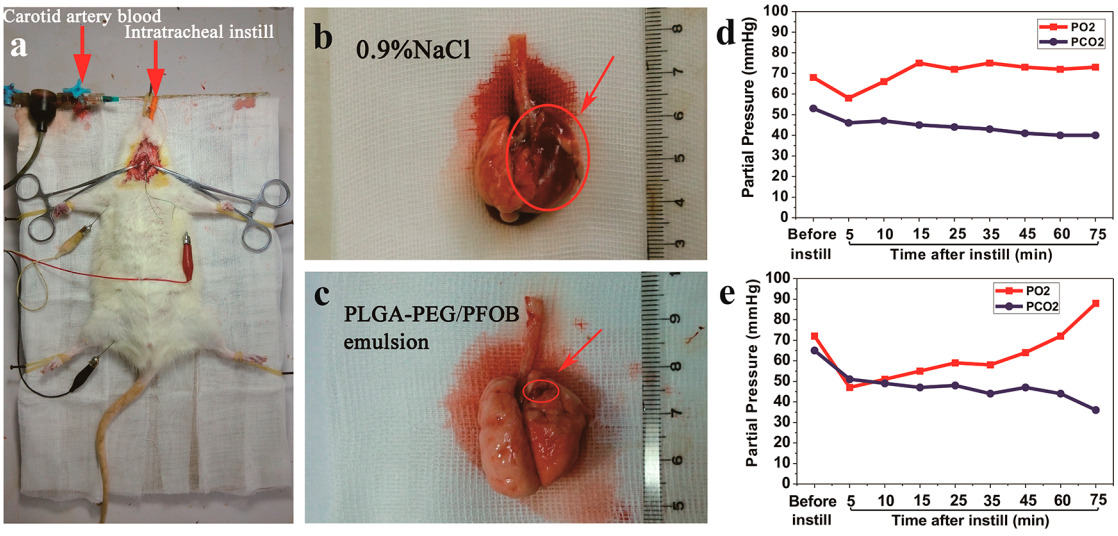

Figure 7. (a) *In vivo* experiment of PLGA-PEG/PFOB emulsion, lungs of rats instilled with (b) 0.9% NaCl and (c) PLGA-PEG/PFOB emulsion and the changes of PO_2 and PCO_2 of rats instilled with (d) 0.9% NaCl and (e) PLGA-PEG/PFOB emulsion.

DOI: 10.1021/acsami.5b04226
ACS Appl. Mater. Interfaces 2015, 7, 18369–18378

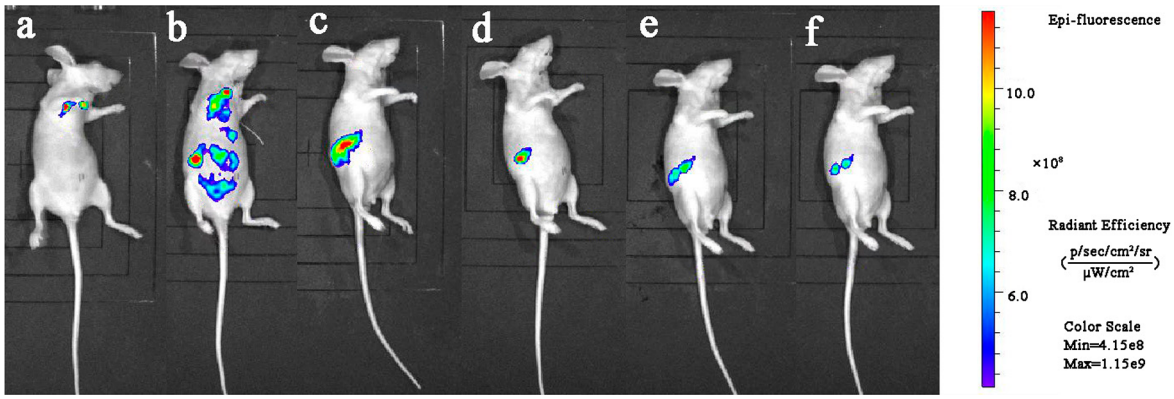

Figure 8. *In vivo* biodistribution of PLGA-PEG/PFOB emulsion after pulmonary delivery at times of (a) 0, (b) 1, (c) 2, (d) 3, (e) 4, and (f) 5 h.

PFOB slowly being released. Moreover, compared to the control group, PCO_2 of the experimental group has a more dramatic decline, which can be explained by the fact that the high dissolved CO_2 ability of PFOB helps rats emit CO_2 more quickly. Therefore, the changes of PO_2 and PCO_2 indicate PLGA-PEG/PFOB emulsion can supply oxygen to rats and improve rats' lung ventilation.

To evaluate the biodistribution and metabolism of PLGA-PEG/PFOB emulsion in vivo, PLGA-FITC was used as a marker to monitor the trace of PLGA-PEG/PFOB emulsion. A PLGA-PEG/PLGA-FITC/PFOB emulsion was prepared and then instilled into some nude mice to observe distribution in different organs. Finally, the mice were anatomized to confirm the organ type. As shown in Figure 8a, after the mice were instilled with 0.05 mL of the emulsion through trachea, the emulsion is deposited in lung and bronchus. However, the emulsion was spread in many organs after 1 h of administration (Figure 8b), such as lung, heart, liver, bowel, and kidney, which may be attributed to their diffusing along with blood flow. Closer observation reveals that there is the most content in kidney. Furthermore, with the time increasing to 2 h (Figure 8c), the color around kidney becomes more and more red, which implies the emulsion is concentrated to the kidney. However, the content in kidney is decreased gradually after an administration time from 3 to 5 h, which shows that the emulsion may be metabolized. The above results indicate that the PLGA-PEG/PFOB emulsion could distribute in most internal organs through blood flow after pulmonary delivery and finally metabolized through kidney.

CONCLUSION

The NH_2-PEG-COOH is successfully conjugated with PLGA-COOH at a grafting ratio of 90%. TEM, DLS, and FT-IR show that PFOB emulsion with a nanosize encapsulated in PLGA-PEG could be obtained, and cell cytotoxicity shows its good biocompatibility. Furthermore, cell hypoxia-reoxygenation experiment reveals that cell viability has a significant enhancement after reoxygenation with PLGA-PEG/PFOB emulsion because of the sufficient and timely oxygen supply. Meanwhile, hypoxia-reoxygenation injury will happen along with cell reoxygenation, which is reflected by increasing ROS in cells. However, the integration of intracellular ROS and cell viability implies that this degree of hypoxia-reoxygenation injury is sublethal to HCT116 cells when the concentration of PLGA-PEG/PFOB emulsion is lower than 0.2 mg/mL. The change of the expression level of HIF-1α is similar to cell viability during reoxygenation, which suggests HIF-1α or its downstream proteins may make a significant contribution to cell viability. *In vivo* oxygen supply was assessed in rats through pulmonary delivery, which shows that PLGA-PEG/PFOB emulsion can supply oxygen to rats and improve rats' lungs ventilation. *In vivo* biodistribution of PLGA-PEG/PLGA-FITC/PFOB emulsion shows that the PLGA-PEG/PFOB emulsion could distribute in most internal organs through blood flow after pulmonary delivery and finally metabolized through kidney.

AUTHOR INFORMATION

Corresponding Authors

*E-mail: yzjzhu@163.com.
*E-mail: linzhaofen@sina.com.
*E-mail: hdn_nercn@163.com.

Author Contributions

$^{\nabla}$These authors contributed equally to this work.

Notes

The authors declare no competing financial interest.

ACKNOWLEDGMENTS

The work is supported by National Key Technology Research and Development Program (no. 2014BAK05B02), National Natural Science Foundation of China (nos. 51303135 and 81172309), and Minhang District Science and Technology Project (no. 2014MH089).

REFERENCES

(1) Agashe, H.; Lagisetty, P.; Awasthi, S.; Awasthi, V. Improved Formulation of Liposome-Encapsulated Hemoglobin with an Anionic Non-Phospholipid. *Colloids Surf., B* **2010**, *75*, 573−583.

(2) Bauer, J.; Zahres, M.; Zellermann, A.; Kirsch, M.; Petrat, F.; de Groot, H.; Mayer, C. Perfluorocarbon-Filled Poly(lactide-co-gylcolide) Nano- and Microcapsules as Artificial Oxygen Carriers for Blood Substitutes: a Physico-Chemical Assessment. *J. Microencapsulation* **2010**, *27*, 122−132.

(3) Freire, M. G.; Dias, A. M. A.; Coutinho, J. A. P.; Coelho, M. A. Z.; Marrucho, I. M. Enzymatic Method for Determining Oxygen Solubility in Perfluorocarbon Emulsions. *Fluid Phase Equilib.* **2005**, *231*, 109−113.

(4) Goh, F. The Use of Perfluorocarbons in Encapsulated Cell Systems: Their Effect on Cell Viability and Function and Their Use in Noninvasively Monitoring the Cellular Microenvironment. Ph.D. Dissertation, Georgia Institute of Technology, 2011.

(5) Jouan-Hureaux, V.; Audonnet-Blaise, S.; Lacatusu, D.; Krafft, M. P.; Dewachter, P.; Cauchois, G.; Stoltz, J. F.; Longrois, D.; Menu, P. Effects of a New Perfluorocarbon Emulsion on Human Plasma and Whole-Blood Viscosity in the Presence of Albumin, Hydroxyethyl

DOI: 10.1021/acsami.5b04226
ACS Appl. Mater. Interfaces 2015, 7, 18369−18378

Starch, or Modified Fluid Gelatin: an In Vitro Rheologic Approach. *Transfusion* **2006**, *46*, 1892−1898.
(6) Riess, J. G. Understanding the Fundamentals of Perfluorocarbons and Perfluorocarbon Emulsions Relevant to In Vivo Oxygen Delivery. *Artif. Cells, Blood Substitutes, Biotechnol.* **2005**, *33*, 47−63.
(7) Jia, X.; Cai, X.; Chen, Y.; Wang, S.; Xu, H.; Zhang, K.; Ma, M.; Wu, H.; Shi, J.; Chen, H. Perfluoropentane-Encapsulated Hollow Mesoporous Prussian Blue Nanocubes for Activated Ultrasound Imaging and Photothermal Therapy of Cancer. *ACS Appl. Mater. Interfaces* **2015**, *7*, 4579−4588.
(8) Kaneda, M. M.; Caruthers, S.; Lanza, G. M.; Wickline, S. A. Perfluorocarbon Nanoemulsions for Quantitative Molecular Imaging and Targeted Therapeutics. *Ann. Biomed. Eng.* **2009**, *37*, 1922−1933.
(9) Marsh, J. N.; Partlow, K. C.; Abendschein, D. R.; Scott, M. J.; Lanza, G. M.; Wickline, S. A. Molecular Imaging with Targeted Perfluorocarbon Nanoparticles: Quantification of the Concentration Dependence of Contrast Enhancement for Binding to Sparse Cellular Epitopes. *Ultrasound Med. Biol.* **2007**, *33*, 950−958.
(10) Pisani, E.; Tsapis, N.; Galaz, B.; Santin, M.; Berti, R.; Taulier, N.; Kurtisovski, E.; Lucidarme, O.; Ourevitch, M.; Doan, B. T.; Beloeil, J. C.; Gillet, B.; Urbach, W.; Bridal, S. L.; Fattal, E. Perfluorooctyl Bromide Polymeric Capsules as Dual Contrast Agents for Ultrasonography and Magnetic Resonance Imaging. *Adv. Funct. Mater.* **2008**, *18*, 2963−2971.
(11) Sheeran, P. S.; Luois, S.; Dayton, P. A.; Matsunaga, T. O. Formulation and Acoustic Studies of a New Phase-Shift Agent for Diagnostic and Therapeutic Ultrasound. *Langmuir* **2011**, *27*, 10412−10420.
(12) Brandhorst, D.; Iken, M.; Brendel, M. D.; Bretzel, R. G.; Brandhorst, H. Successful Pancreas Preservation by a Perfluorocarbon-Based One-Layer Method For Subsequent Pig Islet Isolation. *Transplantation* **2005**, *79*, 433−437.
(13) Marada, T.; Zacharovova, K.; Saudek, F. Perfluorocarbon Improves Post-Transplant Survival and Early Kidney Function following Prolonged Cold Ischemia. *Eur. Surg. Res.* **2010**, *44*, 170−178.
(14) Matsumoto, S.; Kuroda, Y. Perfluorocarbon for Organ Preservation before Transplantation. *Transplantation* **2002**, *74*, 1804−1809.
(15) Arab, A.; Kuemmerer, K.; Wang, J.; Bode, C.; Hehrlein, C. Oxygenated Perfluorochemicals Improve Cell Survival during Reoxygenation by Pacifying Mitochondrial Activity. *J. Pharmacol. Exp. Ther.* **2008**, *325*, 417−424.
(16) Guzy, R. D.; Hoyos, B.; Robin, E.; Chen, H.; Liu, L.; Mansfield, K. D.; Simon, M. C.; Hammerling, U.; Schumacker, P. T. Mitochondrial Complex III is Required for Hypoxia-Induced ROS Production and Cellular Oxygen Sensing. *Cell Metab.* **2005**, *1*, 401−408.
(17) Hsieh, C. H.; Kuo, J. W.; Lee, Y. J.; Chang, C. W.; Gelovani, J. G.; Liu, R. S. Construction of Mutant TKGFP for Real-Time Imaging of Temporal Dynamics of HIF-1 Signal Transduction Activity Mediated by Hypoxia and Reoxygenation in Tumors in Living Mice. *J. Nucl. Med.* **2009**, *50*, 2049−2057.
(18) Li, C.; Jackson, R. M. Reactive Species Mechanisms of Cellular Hypoxia-Reoxygenation Injury. *Am. J. Physiol.: Cell Physiol.* **2002**, *282*, C227−C241.
(19) Li, S.; Tabar, S. S.; Malec, V.; Eul, B. G.; Klepetko, W.; Weissmann, N.; Grimminger, F.; Seeger, W.; Rose, F.; Hanze, J. NOX4 Regulates ROS Levels under Normoxic and Hypoxic Conditions, Triggers Proliferation, and Inhibits Apoptosis in Pulmonary Artery Adventitial Fibroblasts. *Antioxid. Redox Signaling* **2008**, *10*, 1687−1698.
(20) Luo, L.; Lu, J.; Wei, L.; Long, D.; Guo, J. Y.; Shan, J.; Li, F. S.; Lu, P. Y.; Li, P. Y.; Feng, L. The Role of HIF-1 in Up-Regulating MICA Expression on Human Renal Proximal Tubular Epithelial Cells during Hypoxia/Reoxygenation. *BMC Cell Biol.* **2010**, *11*, 91.
(21) Shao, Z. H.; Li, C. Q.; Vanden Hoek, T. L.; Becker, L. B.; Schumacker, P. T.; Wu, J. A.; Attele, A. S.; Yuan, C. S. Extract from Scutellaria Baicalensis Georgi Attenuates Oxidant Stress in Cardiomyocytes. *J. Mol. Cell. Cardiol.* **1999**, *31*, 1885−1895.
(22) Mansour, H. M.; Rhee, Y. S.; Wu, X. Nanomedicine in Pulmonary Delivery. *Int. J. Nanomed.* **2009**, *4*, 299−319.
(23) Sharma, R.; Corcoran, T. E.; Garoff, S.; Przybycien, T. M.; Swanson, E. R.; Tilton, R. D. Quasi-Immiscible Spreading of Aqueous Surfactant Solutions on Entangled Aqueous Polymer Solution Subphases. *ACS Appl. Mater. Interfaces* **2013**, *5*, 5542−5549.
(24) Smola, M.; Vandamme, T.; Sokolowski, A. Nanocarriers as Pulmonary Drug Delivery Systems to Treat and to Diagnose Respiratory and non Respiratory Diseases. *Int. J. Nanomed.* **2008**, *3*, 1−19.
(25) Ungaro, F.; d'Angelo, I.; Miro, A.; La Rotonda, M. I.; Quaglia, F. Engineered PLGA Nano- and Micro-Carriers for Pulmonary Delivery: Challenges and Promises. *J. Pharm. Pharmacol.* **2012**, *64*, 1217−1235.
(26) Secret, E.; Kelly, S. J.; Crannell, K. E.; Andrew, J. S. Enzyme-Responsive Hydrogel Microparticles for Pulmonary Drug Delivery. *ACS Appl. Mater. Interfaces* **2014**, *6*, 10313−10321.
(27) Takami, T.; Murakami, Y. Development of PEG-PLA/PLGA Microparticles for Pulmonary Drug Delivery Prepared by a Novel Emulsification Technique Assisted with Amphiphilic Block Copolymers. *Colloids Surf., B* **2011**, *87*, 433−438.
(28) Yang, Y.; Bajaj, N.; Xu, P.; Ohn, K.; Tsifansky, M. D.; Yeo, Y. Development of Highly Porous Large PLGA Microparticles for Pulmonary Drug Delivery. *Biomaterials* **2009**, *30*, 1947−1953.
(29) Martín-Banderas, L.; Angeles Holgado, M.; Álvarez-Fuentes, J.; Fernández-Arévalo, M. Use of Flow Focusing® Technology to Produce Tobramycin-Loaded PLGA Microparticles for Pulmonary Drug Delivery. *Med. Chem.* **2012**, *8*, 533−549.
(30) Yoneki, N.; Takami, T.; Ito, T.; Anzai, R.; Fukuda, K.; Kinoshita, K.; Sonotaki, S.; Murakami, Y. One-Pot Facile Preparation of PEG-Modified PLGA Nanoparticles: Effects of PEG and PLGA on Release Properties of the Particles. *Colloids Surf., A* **2015**, *469*, 66−72.
(31) HIRSCHL, R. B.; CROCE, M.; GORE, D.; WIEDEMANN, H.; DAVIS, K.; ZWISCHENBERGER, J.; BARTLETT, H. Prospective, Randomized, Controlled Pilot Study of Partial Liquid Ventilation in Adult Acute Respiratory Distress Syndrome. *Am. J. Respir. Crit. Care Med.* **2002**, *165*, 781−787.
(32) Wolf, G. K.; Sheeran, P.; Heitz, D.; Thompson, J. E.; Arnold, J. H. Gas Exchange and Lung Mechanics during High Frequency Ventilation in the Perflubron-Treated Lung. *Pediatr. Crit. Care Med.* **2008**, *9*, 641−646.
(33) Doctor, A.; Al-Khadra, E.; Tan, P.; Watson, K. F.; Diesen, D. L.; Workman, L. J.; Thompson, J. E.; Rose, C. E.; Arnold, J. H. Extended High-Frequency Partial Liquid Ventilation in Lung Injury: Gas Exchange, Injury Quantification, and Vapor Loss. *J. Appl. Physiol.* **2003**, *95*, 1248−1258.
(34) Pisani, E.; Tsapis, N.; Paris, J.; Nicolas, V.; Cattel, L.; Fattal, E. Polymeric Nano/Microcapsules of Liquid Perfluorocarbons for Ultrasonic Imaging: Physical Characterization. *Langmuir* **2006**, *22*, 4397−4402.
(35) Cheng, J.; Teply, B.; Sherifi, I.; Sung, J.; Luther, G.; Gu, F.; Levynissenbaum, E.; Radovicmoreno, A.; Langer, R.; Farokhzad, O. Formulation of Functionalized PLGA-PEG Nanoparticles for In Vivo Targeted Drug Delivery. *Biomaterials* **2007**, *28*, 869−876.
(36) Diaz-Lopez, R.; Tsapis, N.; Santin, M.; Bridal, S. L.; Nicolas, V.; Jaillard, D.; Libong, D.; Chaminade, P.; Marsaud, V.; Vauthier, C.; Fattal, E. The Performance of PEGylated Nanocapsules of Perfluorooctyl Bromide as an Ultrasound Contrast Agent. *Biomaterials* **2010**, *31*, 1723−1731.
(37) Wang, Z.; Ting, Z.; Li, Y.; Chen, G.; Lu, Y.; Hao, X. MicroRNA-199a is Able to Reverse Cisplatin Resistance in Human Ovarian Cancer Cells Through the Inhibition of Mammalian Target of Rapamycin. *Oncol. Lett.* **2013**, *6*, 789−794.
(38) Wu, Z. B.; Cai, L.; Lin, S. J.; Xiong, Z. K.; Lu, J. L.; Mao, Y.; Yao, Y.; Zhou, L. F. High-Mobility Group Box 2 is Associated with Prognosis of Glioblastoma by Promoting Cell Viability, Invasion, and Chemotherapeutic Resistance. *Neuro-oncology* **2013**, *15*, 1264−1275.
(39) Yang, L.; Wu, X. H.; Wang, D.; Luo, C. L.; Chen, L. X. Bladder Cancer Cell-Derived Exosomes Inhibit Tumor Cell Apoptosis and Induce Cell Proliferation In Vitro. *Mol. Med. Rep.* **2013**, *8*, 1272−1278.

DOI: 10.1021/acsami.5b04226
ACS Appl. Mater. Interfaces 2015, 7, 18369−18378

(40) Yamada, J.; Yoshimura, S.; Yamakawa, H.; Sawada, M.; Nakagawa, M.; Hara, S.; Kaku, Y.; Iwama, T.; Naganawa, T.; Banno, Y.; Nakashima, S.; Sakai, N. Cell Permeable ROS Scavengers, Tiron and Tempol, Rescue PC12 Cell Death Caused by Pyrogallol or Hypoxia/Reoxygenation. *Neurosci. Res.* **2003**, *45*, 1−8.
(41) NG, C. K.; DESHPANDE, S. S.; IRANI, K.; ALEVRIADOU, B. R. Adhesion of Flowing Monocytes to Hypoxia-Reoxygenation-Exposed Endothelial Cells Role of Rac1, ROS, and VCAM-1. *Am. J. Physiol.: Cell Physiol.* **2002**, *283*, C93−C102.
(42) Millar, T. M.; Phan, V.; Tibbles, L. A. ROS Generation in Endothelial Hypoxia and Reoxygenation Stimulates MAP Kinase Signaling and Kinase-Dependent Neutrophil Recruitment. *Free Radical Biol. Med.* **2007**, *42*, 1165−1177.
(43) Toffoli, S.; Roegiers, A.; Feron, O.; Van Steenbrugge, M.; Ninane, N.; Raes, M.; Michiels, C. Intermittent Hypoxia is an Angiogenic Inducer for Endothelial Cells: Role of HIF-1. *Angiogenesis* **2009**, *12*, 47−67.
(44) Martinez-Romero, R.; Canuelo, A.; Martinez-Lara, E.; Javier Oliver, F.; Cardenas, S.; Siles, E. Poly(ADP-Ribose) Polymerase-1 Modulation of In Vivo Response of Brain Hypoxia-Inducible Factor-1 to Hypoxia/Reoxygenation is Mediated by Nitric Oxide and Factor Inhibiting HIF. *J. Neurochem.* **2009**, *111*, 150−159.

DOI: 10.1021/acsami.5b04226
ACS Appl. Mater. Interfaces 2015, 7, 18369−18378